AAPS PharmSciTech (2023) 24:84
https://doi.org/10.1208/s12249-023-02529-4

RESEARCH ARTICLE

Evaluation and Screening of Biopharmaceuticals using Multi-Angle Dynamic Light Scattering

Ashutosh Sharma[1] · Jason Beirne[2] · Dikshitkumar Khamar[2] · Ciaran Maguire[3] · Ambrose Hayden[1] · Helen Hughes[1]

Received: 1 November 2022 / Accepted: 9 February 2023 / Published online: 22 March 2023

Abstract

Biopharmaceuticals are large, complex and labile therapeutic molecules prone to instability due to various factors during manufacturing. To ensure their safety, quality and efficacy, a wide range of critical quality attributes (CQAs) such as product concentration, aggregation, particle size, purity and turbidity have to be met. Size exclusion chromatography (SEC) is the gold standard to measure protein aggregation and degradation. However, other techniques such as dynamic light scattering (DLS) are employed in tandem to measure the particle size distribution (PSD) and polydispersity of biopharmaceutical formulations. In this study, the application of multi-angle dynamic light scattering (MADLS) was evaluated for the determination of particle size, particle concentration and aggregation in 3 different protein modalities, namely bovine serum albumin (BSA) and two biopharmaceuticals including a monoclonal antibody (mAb) and an enzyme. The obtained calibration curve ($R^2 > 0.95$) for the particle number concentration of the 3 proteins and the observed correlation between MADLS and SEC ($R^2 = 0.9938$) for the analysis of aggregation in the enzyme can be employed as a 3-in-1 approach to assessing particle size, concentration and aggregation for the screening and development of products while also reducing the number of samples and experiments required for analysis prior to other orthogonal tests.

Keywords biopharmaceutical characterization · biopharmaceuticals · dynamic light scattering · size exclusion chromatography · spectroscopy

Abbreviations

BSA	Bovine serum albumin
CQAs	Critical quality attributes
DCR	Derived mean count rate
DLS	Dynamic light scattering
HMWS	High molecular weight species
HPLC	High-performance liquid chromatography
mAb	Monoclonal antibody
MS	Mass spectrometry
MADLS	Multi-angle dynamic light scattering
PAT	Process analytical technology
PDI	Polydispersity index
PSD	Particle size distribution
QC	Quality control
RSD	Relative standard deviation
SEC	Size exclusion chromatography
UHPLC	Ultra high-performance liquid chromatography
UV-Vis	Ultraviolet-visible light spectroscopy

✉ Ashutosh Sharma
ashutosh.sharma@postgrad.wit.ie

✉ Helen Hughes
helen.hughes@setu.ie

[1] Pharmaceutical and Molecular Biotechnology Research Centre (PMBRC), South East Technological University (SETU), Main Campus, Cork Road, Waterford X91 K0EK, Ireland

[2] Manufacturing Science, Analytics and Technology (MSAT), Sanofi, IDA Industrial Park, Waterford X91 TP27, Ireland

[3] Particular Sciences Ltd, Rosemount Business Park, Ballycoolin D11 T327, Dublin, Ireland

Introduction

It is well-known that proteins are sensitive molecules and susceptible to physical and chemical instability resulting in aggregation, denaturation, etc. [1–4]. Protein aggregation is one of the critical quality attributes (CQAs) that can lead to increased immunogenicity and decreased product efficacy [5] though in some cases dimerization and oligomerization can be integral to protein activity [6]. To ensure the safety, quality and efficacy of these products as per the International Council for Harmonisation (ICH) guidelines and current good manufacturing practices (cGMP), various

analytical and characterization techniques are employed prior to batch release [7]. Historically, several methods such as Bradford protein assay, bicinchoninic acid (BCA), Lowry's assay and other dye-based methods have been used to assess protein concentration. However, the drawbacks associated with these methods include the requirement for additional reagents, sample preparation, compatibility with sample type, interference from multiple absorbing species and analysis time [8, 9]. Currently, UV–Vis spectroscopy and chromatographic methods including reversed-phase high-performance liquid chromatography (RP-HPLC) and size exclusion chromatography (SEC) are the quality control (QC) release tests for concentration, purity, aggregation and degradation [10]. However, the chromatographic methods are destructive techniques which typically require long equilibration and analysis times, while there is a requirement for additional reagents and consumables, including buffers and columns. Although some ultra high-performance liquid chromatographic (UHPLC) methods can have shorter run times, method development and validation for each product and different formulations are time consuming. Even though SEC employs mild isocratic and elution conditions that confer minimal impact on the conformational stability, protein aggregates with weak intermolecular affinity can dissociate into monomers in the mobile phase [11, 12]. Along with these techniques, several process analytical technologies (PATs) available for product and process characterization have been summarized in literature [7]. Of these, DLS [13], UV–Vis spectroscopy [14], Raman spectroscopy [15, 16], infrared (IR) spectroscopy [17] and flow imaging techniques [18] can be employed to characterize and analyse protein structure and aggregation. These techniques are non-destructive, can reduce analysis time and monitor all individual vials or bulk product with high specificity and reproducibility, thereby speeding up the batch release process.

Multi-angle dynamic light scattering (MADLS) is an improvement in the single-angle DLS technique for the analysis of multimodal size distribution of particles with better resolution in the size range of 0.3 nm–1 µm [19–22]. This method is an indicator of protein aggregation or impurities that may be present [23]. Moreover, parameters such as the interaction parameter (k_D) and the second virial coefficient (B_{22}) are widely used to quantify protein–protein interactions using DLS and static light scattering (SLS) [24]. While there are other methods available such as DLS plate reader, CTech™ SoloVPE® and analytical ultra-centrifugation (AUC) for the determination of particle size, product concentration and aggregation, respectively, multi-angle DLS removes angular dependence and is capable of analysing low sample volumes (20 µL) without the need for extensive method development, additional reagents, information about the molar extinction coefficient and calibration [25].

DLS is based on the principle of Brownian motion and Rayleigh scattering. Brownian motion is characterised by the collisions of different sizes of particles and their subsequent changes in directions and velocities. As a laser is passed through the solution, the incident ray is reflected and scattered in all directions. The energy of the scattered and incident light is the same with no loss of energy; this phenomenon is known as Rayleigh scattering. The autocorrelation function measures the scattered light fluctuations over time. The autocorrelation coefficient is given by Eq. 1 and the hydrodynamic diameter is deduced from the Stokes–Einstein's equation (Eq. 2). Readers are referred to the cited references herein on the detailed theory of DLS [26–28].

$$G(\tau) = 1 + \beta.e^{-2D.q^2.\tau} \tag{1}$$

$$D = \frac{k_B.T}{3\ \pi.\eta.d} \tag{2}$$

where $G(\tau)$ is the autocorrelation function at lag time τ, q is the scattering vector, β is the coherence factor, D is the diffusion coefficient, d is the hydrodynamic diameter, k_B is the Boltzmann constant, T is the temperature and η is the viscosity of the fluid.

In addition, this technique has been demonstrated to measure the particle concentration of nanoparticles [28]. The number of particles is deduced by Eq. 3.

$$N_d = \rho_d.A.L \tag{3}$$

where N_d is the number of particles per mL, ρ_d is the particle concentration distribution, A is the cross-sectional area of the scattering volume and L is the length of the scattering volume.

Previously, correlations between DLS and SEC have been shown by authors [11, 29], though quantification of protein aggregation is hard to achieve by DLS alone. While MADLS along with orthogonal techniques has been employed for the characterization of a wide range of CQAs of adeno-associated viruses (AAVs) and lipid-based nanoparticles (LNPs) [25, 30], polystyrene nanoparticles and extracellular vesicles [31], the 3-in-1 capability of MADLS for the screening of particle size, concentration and aggregation of different protein-based biopharmaceuticals has not been explored. In this study, we evaluated the application of MADLS in tandem with UV–Vis spectroscopy and SEC and provide a 3-in-1 approach for the screening of particle size, particle concentration and protein aggregation for three different proteins. To increase the scope of this study, a generic protein standard, bovine serum albumin (BSA); a high-concentration and high molecular weight monoclonal antibody (mAb); and a low-concentration therapeutic enzyme were selected.

Materials and Methods

Preparation of Solutions

BSA (A9647, heat shock fraction, ≥ 98%) and sodium phosphate monobasic and dibasic were purchased from Merck/Sigma-Aldrich, Ireland. Ten milligrams per millitre of BSA was prepared in 10 mM sodium phosphate buffer at pH 7.2. Sucrose-based formulated drug substances, a low-concentration enzyme (4 mg/mL) and a high-concentration mAb (150 mg/mL), were received from Sanofi, Waterford, Ireland. All protein solutions were filtered using a 0.22-µm cellulose acetate filter.

Treatment of BSA

Five dilutions of BSA were prepared as per Table I. Ten milligrams per millitre of native BSA was heated at temperatures of 65°C for 30 min and 24 h, and at 90°C for 3 h. A mixture of the native (25°C) and the heat-treated (65°C for 24 h) BSA solution in the ratio of 9:1 (900:100 µL) was prepared by pipetting 100 µL of the heat-treated solution to 900 µL of the native solution to make up a final volume of 1 mL. Similarly, mixtures of the native and heat-treated solutions were prepared in the different ratios by volume shown in Table I.

Treatment of the mAb

Ten dilutions of the mAb were prepared as per Table I. Two different concentrations of the mAb at 150 mg/mL and 9.37 mg/mL were heat-treated at a temperature of 65°C for 10 min and 30 min. A mixture of the native (25 °C) and heat-treated (65°C) mAb solution in the ratio of 1:1 (500:500 µL) was prepared by pipetting 500 µL of the heat-treated solution to 500 µL of the native solution to make up a final volume of 1 mL. Similarly, different mixture ratios by volume were prepared as shown in Table I.

Treatment of the Enzyme

Nine dilutions of the enzyme were prepared as per Table I. Four milligrams per millitre of the native enzyme was heat-treated at a temperature of 65°C for 10 min. A mixture of the native (25°C) and heat-treated (65°C) enzyme solution in the

Table I Sample Preparation and Treatment Methods for the analysis of the selected proteins

Protein	Dilutions (mg/mL)	Heat treatment	Mixture ratios by volume of the native and heat-treated solutions (µL)
BSA	10 5 1 0.5 0.1	10 mg/mL at 65°C for 30 min, 65°C for 24 h, 90°C for 2–3 h	900:100 (9:1) 500:500 (1:1) 990:10 (99:1)
mAb	150 75 37.5 18.75 9.37 7 4.68 2.34 1.17 0.58	150 mg/mL and 9.37 mg/mL at 65°C for 10–30 min	500:500 (1:1) 850:150 (17:3) 900:100 (9:1)
Enzyme	4 3 2.5 2 1.5 1.25 1 0.5 0.25	4 mg/mL at 65°C for 7–10 min	990:10 (99:1) 975:25 (39:1) 950:50 (19:1) 850:150 (17:3) 700:300 (7:3) 500:500 (1:1) 300:700 (3:7) 150:850 (3:17)

The different heat-treatment conditions and mixture ratios chosen for the 3 proteins were based on their propensity to aggregate and form polydispersed solutions. The native and heat-treated samples were mixed together to obtain different known ratios by volume of the monomer to aggregate in a defined range for analysis by MADLS

BSA, bovine serum albumin; *mAb*, monoclonal antibody

ratio of 99:1 (990:10 µL) was prepared by pipetting 10 µL of the heat-treated solution to 990 µL of the native solution to make up a final volume of 1 mL. Similarly, different mixture ratios by volume were prepared as shown in Table I.

Multi-Angle Dynamic Light Scattering (MADLS)

All samples were analysed by the Zetasizer Ultra (Malvern Panalytical Ltd.) equipped with a nominally 10-mW He–Ne laser at a wavelength of 633 nm. One millilitre of sample was measured in a 1 cm × 1 cm transparent disposable cuvette. The cell position was set to 4.64 mm to allow for measurement of the sample across all detector angles. All MADLS measurements were collected at 3 different angles of detection, namely, back scatter (174.7°), side scatter (90°) and forward scatter (12.78°) with an equilibration time of 120 s. The refractive index of the protein and water used were 1.45 and 1.33, respectively. The viscosity of the low-concentration dispersant for BSA and the enzyme at 25°C was 0.8872 mPa.s. The viscosity of the high-concentration mAb was corrected using the measured values by rheometry (HAAKE™ MARS™ Rheometer by Thermo Scientific). MADLS data was acquired and processed by the ZS XPLORER software version 1.3.2.27 (Malvern Panalytical Ltd.). The dispersant's scattering mean count rate (kcps) was measured prior to particle concentration measurements.

UV–Vis Spectroscopy

The standard operating UV–Vis test method was used to verify and validate the linearity of the calibration curve for the particle number concentration measurements by MADLS. All protein concentrations were measured in a 1 × 1 cm transparent quartz cuvette by a UV–Vis spectrometer (Spectro Star nano from BMG Labtech) at 280 nm with molar extinction coefficients of 0.67 mL mg^{-1} cm^{-1} (BSA), 1.41 mL mg^{-1} cm^{-1} (mAb) and 2.41 mL mg^{-1} cm^{-1} (enzyme) using Beer-Lambert's law (Eq. 4).

$$A = \varepsilon.C.L \tag{4}$$

where A is the absorbance, ε is the molar extinction coefficient in mL mg^{-1} cm^{-1}, C is the concentration in mg/mL and L is path length in cm.

Size Exclusion Chromatography

The aggregation profile of enzyme samples was determined using high-performance liquid chromatography (HPLC 1260 by Agilent Technologies) with a UV–Vis detector at 280 nm, at a flow rate of 0.5 mL/min through a TSK gel 3000 SWXL column with an injection volume of 20 µL. The mobile phase contained 20 mM sodium phosphate dibasic and 200 mM sodium chloride at pH 6.5. All data were analysed on the Empower Chromatography Data System (Waters™).

Results

Protein Size and Particle Number Concentration Analyses

In this section, MADLS assessment for particle size and concentration measurements was performed to define the operational range, linearity and reproducibility for the three proteins.

BSA

The hydrodynamic diameter of monomeric BSA was measured to be 7.5 nm across a concentration range of 0.1–10 mg/mL with an RSD of 4.5%. While all samples were monomodal with a polydispersity index (PDI) of < 0.2, small artifacts were observed at low concentration in the size range of 20–200 nm but with poor reproducibility. The particle size distribution (PSD) by intensity along with the corresponding correlograms is reported in the supplementary information (SI, Fig. 1). All particle concentration measurements were performed as per section 'Multi-Angle Dynamic Light Scattering (MADLS)'. A coefficient of determination (R^2) of 0.9999 with an average RSD of 22% was obtained between the particle concentration by MADLS and the concentration by UV–Vis spectroscopy (Fig. 1 (a)). This result is well-known and consistent with literature results [28]. The RSD of the particle concentration increased to 30% at low concentrations in the range of 0.1–0.5 mg/mL. Furthermore, it was observed that the RSD of the particle concentration at a concentration of 10 mg/mL was 23.3%. Additionally, an R^2 of 0.9963 with an average RSD of 2.5% obtained between the derived mean count rate (DCR) and the concentration by UV–Vis spectroscopy verified that linearity was maintained within a particle concentration range of 0.1–10 mg/mL (SI, Fig. 5 (a)). Therefore, the calibration curve obtained by MADLS can be used as a quick screening tool to assess the concentration and size of native BSA in tandem with conventional techniques such as UV–Vis spectroscopy.

mAb

The particle size and concentration of the mAb were measured over a wide concentration range of 0.5–150 mg/mL as per Table I. The hydrodynamic diameter of the mAb (9.65 nm) was observed to be consistent within a concentration range of 1.17–37.5 mg/mL with an RSD of 3.6% and PDI < 0.15. The viscosity-corrected hydrodynamic

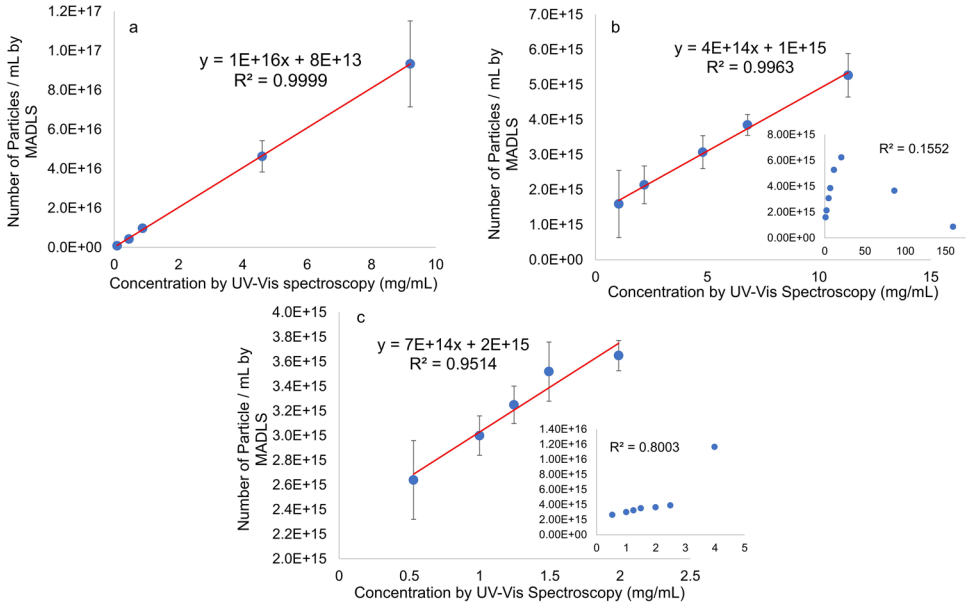

Fig. 1 Particle concentration calibration curve for **a** BSA, **b** mAb and **c** enzyme

diameter at high concentrations of 150 mg/mL (8.23 mPa.s) and 75 mg/mL (2.33 mPa.s) resulted in a lower particle size. The PSD by intensity along with their corresponding correlograms is shown in supplementary information (SI, Fig. 2). The operational particle concentration range between MADLS and UV–Vis spectroscopy was observed in the range of 1.17–9.37 mg/mL with an R^2 of 0.9963 and an average RSD of 24% (Fig. 1 (b)). At high mAb concentrations of ≥ 18 mg/mL, the coefficient of determination significantly dropped to an R^2 of 0.15 represented by the inset reported in Fig. 1 (b). An RSD of up to 60% was observed in the lower concentration range of 1.17–2.34 mg/mL. Additionally, the DCR showed linearity ($R^2 = 0.9887$) and reproducibility (average RSD of 4.8%) with the measured concentration by UV–Vis spectroscopy in the concentration range of 1.17–9.37 mg/mL which verified the linearity of particle concentration (SI, Fig. 5 (b)). Therefore, the calibration curve obtained by MADLS in the operational concentration range can be employed in tandem with orthogonal techniques to assess any aberrations in the size and concentration of the native mAb.

Enzyme

The hydrodynamic diameter of the monomeric enzyme (9.4 nm) was consistent over a concentration range of 0.5–4 mg/mL with an RSD of 8%. A PDI of 0.3 was obtained with a multimodal distribution by intensity. The additional peaks between 20 and 500 nm indicated the presence of high molecular weight species (HMWS) of the enzyme. The RSD of the peaks appearing at 88.9 nm and 400 nm was 10% and 4.3%, respectively, though the peak at 400 nm was only observed at low concentrations as evident from the delay in the gradient of the correlation coefficient at 0.5 mg/mL. The PSD by intensity along with their corresponding correlograms is shown in supplementary information (SI, Fig. 3). The operational particle concentration range between MADLS and UV–Vis spectroscopy was observed to be 0.5–2 mg/mL with an R^2 of 0.9514 and an average RSD of 19% (Fig. 1 (c)). An RSD of ≤ 20% was observed both at lower concentrations in the range of 0.5–1 mg/mL and at higher concentrations of > 2.5 mg/mL above which the correlation curve began to drop with an $R^2 < 0.90$ as represented by the inset in Fig. 1 (c). In this case, the R^2 of the particle concentration obtained was comparatively lower than that of BSA (0.9999) and the mAb (0.9963). Additionally, the DCR was linear ($R^2 = 0.9745$) and reproducible over a concentration range of 0.5–2 mg/mL (SI, Fig. 5 (c)). Therefore, the calibration curve obtained in the operational concentration range for the polydispersed enzyme solution by MADLS can be employed as a screening method to assess any deviations in the size and concentration of the enzyme.

Protein Aggregation Analyses

In this section, MADLS was employed to measure protein aggregation of the three proteins.

BSA

As per section 'BSA', the hydrodynamic diameter of monomeric BSA was measured to be 7.5 nm (Fig. 2 (a)).

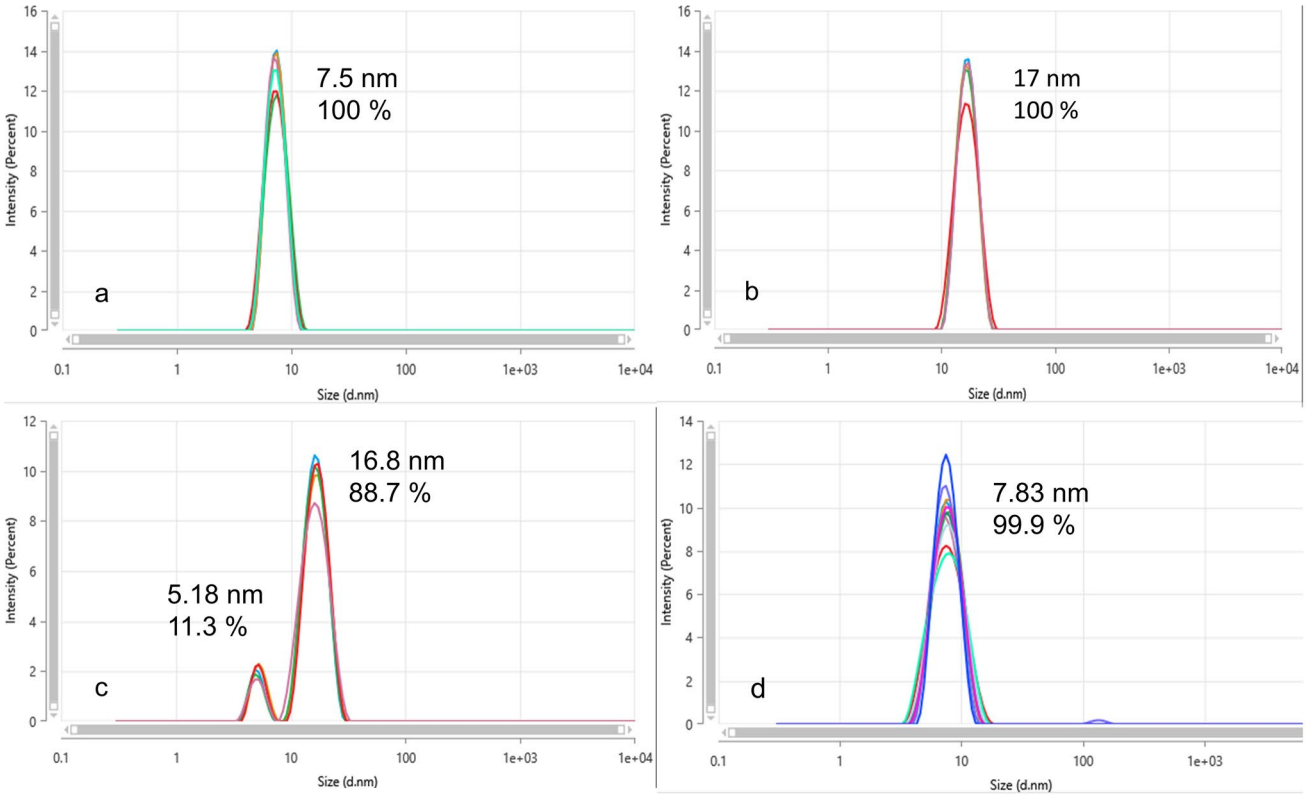

Fig. 2 PSD by intensity of BSA: **a** native at 25°C, **b** at 65°C for 24 h. Mixtures of the native and heat-treated (65°C for 24 h) samples in the ratios of **c** 1:1 (500:500 µL) and **d** 99:1 (990:10 µL). The coloured PSD represent the repeatability of MADLS measurements

Upon heat-treating the protein at 65°C and 90°C, a shift in the particle size was observed at 17 nm (Fig. 2 (b)) and 20 nm (the PSD for 20 nm has not been included in Fig. 2 of this publication), respectively, though the sample remained monomodal (PDI < 0.2) (Fig. 2 (b)). The prepared mixture of the native and the heat-treated (65°C for 24 h) protein in the ratio of 1:1 (500:500 µL) showed the presence of two peaks at 5 and 16 nm (Fig. 2 (c)), respectively. The presence of one additional peak in the sample mixtures (Fig. 2 (c)) indicated the presence of high molecular weight species (HMWS) of BSA as shown by SEC in literature [32, 33], but these aggregation peaks were not observed in all sample mixtures. On increasing the fraction of the native protein in the mixture to 99:1 (990:10 µL), a monodisperse sample (PDI ≤ 0.2) was obtained with a single peak at 7 nm (Fig. 2 (d)). This showed that MADLS analyses were unable to detect and resolve dimers and/or HMWS from the native protein at a low concentration. Therefore, in this case, MADLS would not be the most appropriate technique for the analyses of aggregation of BSA but can be employed as a rapid screening method to detect any deviation in the PSD of the native protein.

mAb

In the operational range, as described in section 'mAb', the hydrodynamic diameter of the mAb was measured to be 9.65 (Fig. 3 (a)). Upon heat-treating the mAb at 65°C for 10 and 30 min, a monomodal distribution was obtained in both cases at 9.37 mg/mL (Fig. 3 (b)), whereas a multimodal distribution by intensity was observed at 150 mg/mL but with poor reproducibility (PDI > 0.2). The PSD for 150 mg/mL has not been included in Fig. 3 of this publication. Moreover, a monomodal distribution was obtained on analysing mixtures of the native and heat-treated samples at different ratios of 1:1 (500:500 µL) and 17:3 (850:150 µL) (Fig. 3 (c) and (d)). This suggested that MADLS was unable to resolve the dimers and/or HMWS and would not be suitable for the analyses of aggregation of the mAb but can be employed as a rapid screening tool to detect any changes in the native mAb PSD.

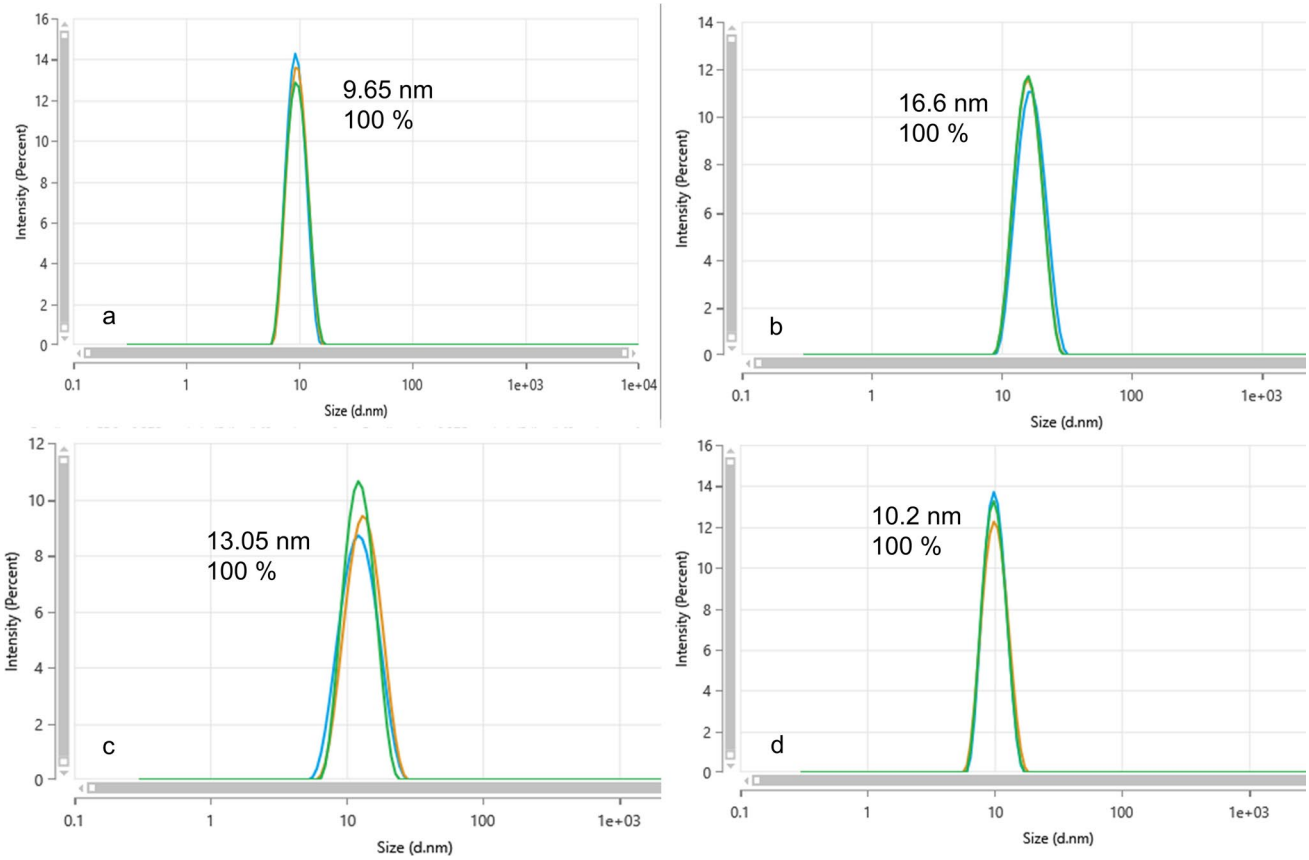

Fig. 3 PSD by intensity of the **a** native mAb at 9.37 mg/mL and **b** 65°C for 10 min at 9.37 mg/mL. Mixtures of the native and heat-treated (65°C for 10 min) mAb in the ratios of **c** 1:1 (500:500 µL) and **d** 17:3 (850:150 µL) at 9.37 mg/mL. The coloured PSD represents the repeatability of MADLS measurements

Enzyme

The hydrodynamic diameter of the monomeric enzyme at 4 mg/mL was observed to be 10.9 nm (RSD = 2.5%) along with a HMWS at 90 nm (RSD = 8%), as shown in Fig. 4 (a). The HMWS peak at 90 nm, confirmed by SEC analyses, was attributed to 'HMWS1' of the enzyme. Upon heat-treating the enzyme at 65°C for 10 min (Fig. 4 (b)), the monomer showed a shift in the particle size (7.9 nm) with a lower intensity distribution of 11.47%, while the particle size of the HMWS1 was significantly lowered to 26.7 nm with an increase in the intensity distribution (88.15%) and an additional minor peak at ~ 400 nm corresponded to 'HMWS2' of the enzyme. An average RSD of < 20% was achieved for the distribution by intensity of the heat-treated sample.

While the monomer, 'HMWS1' and 'HMWS2' of the enzyme were well resolved by MADLS, as the size ratio of each species was greater than a factor of 3, resolution of the dimer was not observed. Nonetheless, to further evaluate the resolution and reproducibility of MADLS measurements of the aggregated samples, a mixture of the native and the heat-treated (65°C for 10 min) solution in the ratio of 99:1 (990:10 µL) (Fig. 4 (c)) showed the presence of 3 distinct peaks at 11 nm, 91.62 nm and 407 nm which were identified as the monomer, 'HMWS1' and 'HMWS2', respectively, by SEC. In this case, an average RSD of < 10% was achieved for the PSD by intensity. Similarly, upon decreasing the fraction of the monomer in the mixtures, a relative decrease and increase in the intensity distribution of the monomer and 'HMWS1', respectively, were observed (Fig. 4 (d)). The relative changes in the intensity distribution for the different ratios of the monomer and 'HMWS1' were confirmed by the corresponding changes in the peak areas by SEC as shown in Fig. 5.

It is important to note that while the resolution of dimers was not observed by MADLS, the concentration of dimers remained < 6% in all samples and did not change significantly as evident from the SEC profile in Fig. 5. Moreover, the presence of 'HMWS2' of the enzyme could not be detected in the different mixtures by SEC as the concentration of 'HMWS2' was below the limit of detection while MADLS was able to detect trace amounts of 'HMWS2' with greater sensitivity due to light scattering.

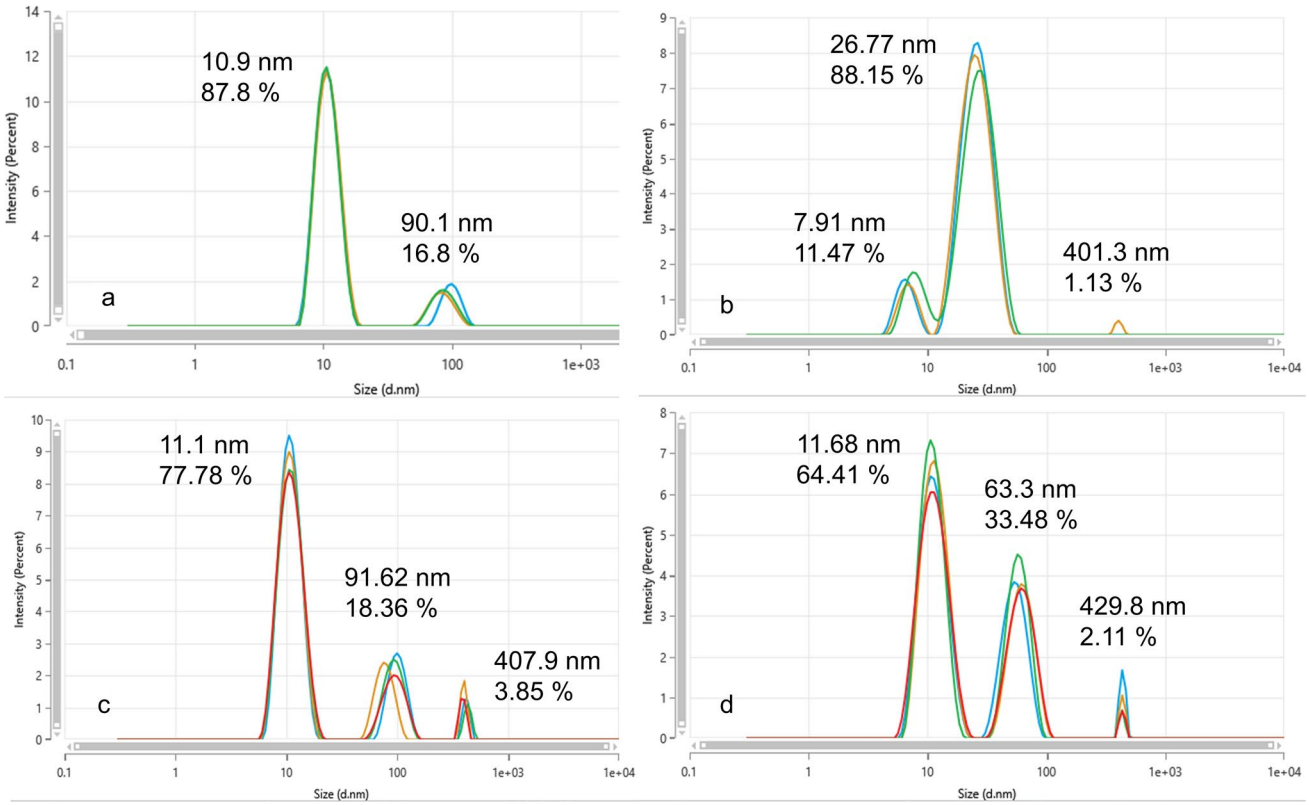

Fig. 4 PSD by intensity of the **a** native enzyme and **b** 65°C for 10 min. Mixtures of the native and heat-treated enzyme (65°C for 10 min) in the ratios of **c** 99:1 (990:10 µL) and **d** 19:1 (950:50 µL). The coloured PSD represents the repeatability of MADLS measurements

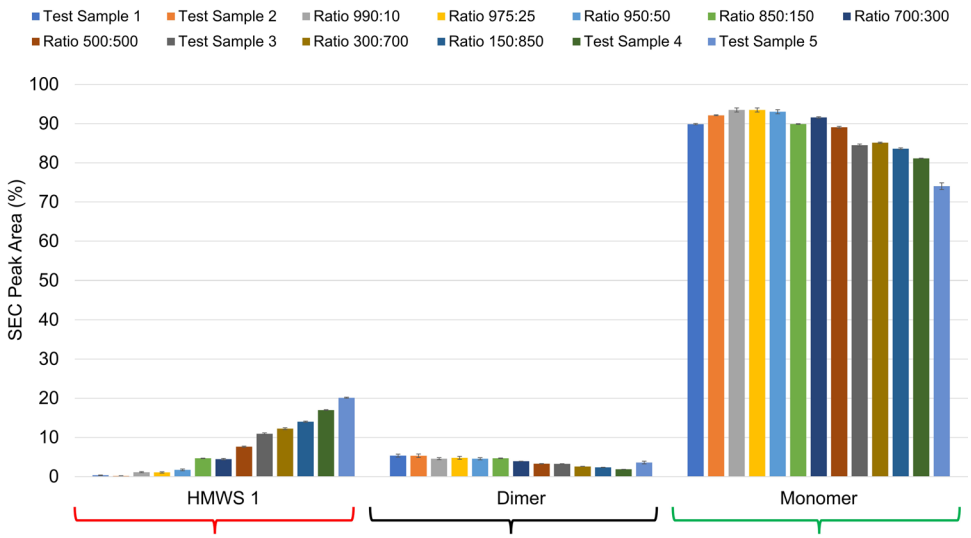

Fig. 5 Aggregation profiles of the different mixture ratios by volume of the monomer and HMWS1 of the enzyme by SEC

Interestingly, a plot between the ratios of the peak areas of the 'HMWS1' and the monomer by SEC *versus* the ratios of the light scattering intensities of the 'HMWS1' and the monomer by MADLS of the prepared mixtures, including 5 unknown test samples, exhibited an excellent quadratic correlation with an R^2 of 0.9938 (Fig. 6). The levels of 'HMWS1' in the enzyme samples are shown in Table II. The level of aggregation increased in the order from zones A to D (Fig. 6). The percentage of 'HMWS1' in test samples 1 and 2 was in the range of 0.1–2%, whereas that in test sample 3 was between 10 and 14% and in test samples 4 and 5 was in the range of 15–20%.

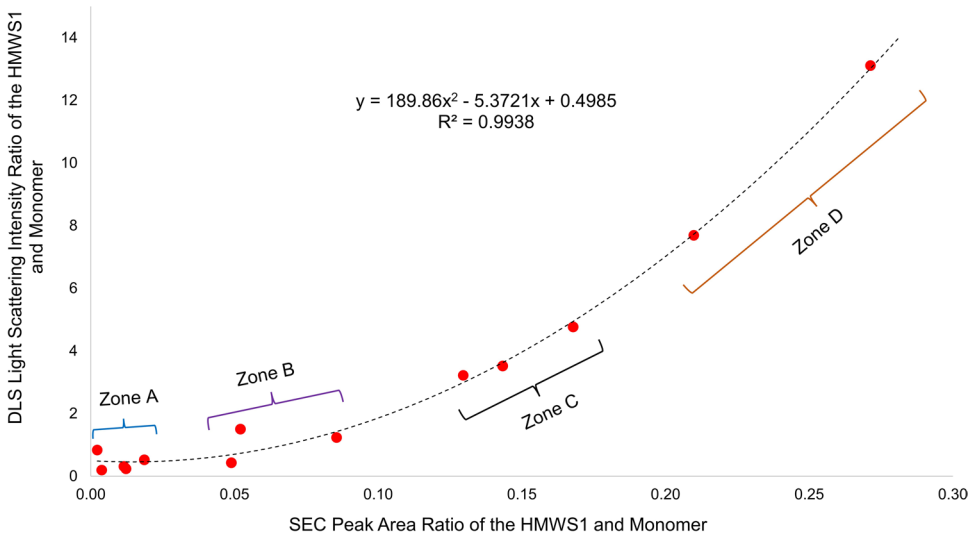

Fig. 6 A quadratic correlation between the peak area ratios of the HMWS1 and monomer by SEC and the light scattering intensity ratios of the HMWS1 and monomer by MADLS of the enzyme

Table II Obtained Levels of HMWS1 in the Enzyme Samples

Zone	Sample	SEC ratio (HMWS1:Monomer)	DLS ratio (HMWS1:Monomer)	Level of HMWS1 (%)
A (Blue)	99:1 (990:10 µL)	0.0123	0.2341	0.1–2
	39:1 (975:25 µL)	0.0116	0.3101	
	19:1 (950:50 µL)	0.0187	0.5202	
	Test sample 1	0.0038	0.1922	
	Test sample 2	0.0023	0.8305	
B (Purple)	17:3 (850:150 µL)	0.0521	1.5000	3–8
	7:3 (700:300 µL)	0.0489	0.4301	
	1:1 (500:500 µL)	0.0855	1.2344	
C (Black)	3:7 (300:700 µL)	0.1433	3.5180	10–14
	3:17 (150:850 µL)	0.1679	4.7630	
	Test sample 3	0.1296	3.2161	
D (Orange)	Test sample 4	0.2098	7.6852	15–20
	Test sample 5	0.2714	13.1030	

SEC, size exclusion chromatography; *DLS*, dynamic light scattering

Discussion

Protein Size

The observed hydrodynamic diameter of BSA was in agreement with the reported values [34, 35], whereas the hydrodynamic diameters of the mAb and enzyme were consistent within the operational concentration range. In the case of the mAb, lowering of particle size at high concentrations of 150 mg/mL and 75 mg/mL occurred as a result of multiple scattering. At high concentrations, multiple scattering results in a decrease in the particle size [28, 36, 37]. The phenomenon of multiple scattering occurs wherein the probability of re-scattering of the scattered photon increases, thereby decreasing the accuracy of particle size measurements. Moreover, an increase in the decay time in the correlation coefficient at higher concentrations explained the diffusion behaviour of the mAb particles at higher viscosities (SI, Fig. 2 (b)). In the case of the enzyme, while the accuracy of size measurements of multimodal distributions decreases due to multiple scattering as well as molecular crowding and restricted diffusion, an RSD of $\leq 10\%$ was achieved for the size measurements of all the multimodal peaks of the enzyme showing reduced peak widths and improved resolution and reproducibility compared to single-angle DLS measurements as shown in supplementary information (SI, Fig. 4).

Particle Number Concentration

In terms of the particle concentration measurements, an R^2 of > 0.95 achieved between UV–Vis spectroscopy and MADLS defined the operating particle concentration range for all the proteins which was verified by the DCR. The increase in the uncertainty of particle concentration measurements for all the proteins at low and high concentrations is attributed to particle number fluctuations and multiple scattering, respectively, which was also reported for gold, silica and polystyrene nanoparticles [28]. This represents the lower and upper limit of the operating particle concentration range of the nanoparticle [26, 28]. Particle number fluctuations arise due to an insufficient number of particles present in the scattering volume wherein the amplitude distribution of the scattered particles does not follow a Gaussian distribution [38]. Moreover, a change in the dynamic equilibrium between the buffer molecules adsorbed at the surface of the protein and those dispersed in the solution may contribute to the increase in the RSD of the particle number measurements [28]. Authors have reported an RSD of 80% in the particle concentration measurements of agglomerated SiO_2 nanoparticles at high concentration and an RSD of up to 30% at low concentration [28], which is consistent with the results shown in section 'Protein Size and Particle Number Concentration Analyses'. As evident from the case of the enzyme, it is important to note that many protein solutions are not completely monodisperse as they may contain low concentrations of dimers/oligomers in dynamic equilibrium with monomers, which also play a role in increasing the uncertainty in measurements. Additionally, other factors such as restricted diffusion, electrostatic repulsion and reversible self-associations must also be considered to account for the error in particle size and concentration measurements [36].

Overall, the concentration calibration curve can be employed for the rapid screening of any deviations in both the product concentration and particle size in tandem with conventional techniques such as UV–Vis spectroscopy.

Protein Aggregation

The ability of MADLS to detect and resolve protein aggregates in heat-treated samples of BSA, the mAb and the enzyme was selective and dependent on the size ratio, nature and relative concentrations of the monomer and the aggregates in the solution. In the case of BSA, a significant shift in the peak size from 7.5 to 20 nm of the heat-treated samples indicated the presence of dimers and/or HMWS, but a resolution of the monomer, dimer, and trimer was not observed distinctly as achieved by SEC [32]. A bimodal distribution of peaks was only observed in the mixtures with HMWS > 10% by volume. Similarly, in the case of the mAb, a shift in the monomodal peak from 9.65 to 22.38 nm indicated the presence of HMWS, but bimodal distributions were observed in only 2 heat-treated samples at 150 mg/mL with poor resolution, reproducibility and accuracy. The skewed particle sizes of the bimodal distributions of BSA and the mAb are attributed to multiple scattering by the presence of multiple species. Also, the absence of the monomer peak in both heat-treated BSA and mAb suggests that the monomer peak was masked by the signals from the HMWS peak. Moreover, the absence of HMWS peaks in the mixtures could suggest the dissociation of HMWS into monomers at low concentrations [11]. Nonetheless, SEC is required to determine the complete aggregation profile of the two proteins. Therefore, the poor resolution and reproducibility of the multimodal measurements for these cases show that MADLS would not be the most appropriate method for the analyses of aggregation of BSA and the mAb but can be employed as a rapid screening tool to detect any changes in the native PSD of these proteins.

In the case of the heat-treated enzyme, improved resolution and reproducibility were achieved between the monomer and the aggregates for the samples containing aggregates < 50% by volume. At higher aggregate concentrations, the light scattering signals from the aggregates dominated the monomer peak and so, MADLS struggled to completely resolve the conjoining peaks. Conversely, a resolution between 20 nm and < 200 nm particles could not be achieved by single-angle DLS [39]. A reduction in particle size of the 10.9 nm peak to 7.9 nm (referred to as the monomer peak) may be due to the conversion of dimers to higher order aggregates. DLS is fundamentally not a high-resolution technique, and as such cannot distinguish between monomers and dimers. In some cases, the peak attributed to monomers also comprises dimers, resulting in the peak mean being skewed towards a larger particle size [28]. These dimers may subsequently form higher order aggregates, removing them from this population mode in the distribution. Upon the formation of these aggregates, the peak corresponding to monomers moved back towards smaller particle size, resulting in both a decrease in particle size for this mode and a reduction in light scattering intensity. Additionally, localised changes in viscosity can be a result of cross-linking or mesh-like network formation of HMWS [40]. Localised changes in viscosity can result in phenomena such as hindered or restricted diffusion. These effects can result in particles being measured larger than expected due to reduced Brownian motion as a consequence of being in localised high viscosity areas. It is important to note that MADLS could not resolve monomer–dimer species of the selected protein nanoparticles in this study, and therefore, unless an alternative analysis procedure is used, the technique is unlikely to be useful in resolving monomer–dimer species in pharmaceutical-grade formulations, which typically have dimer levels ≤ 8%.

The presence of a quadratic correlation between MADLS and SEC for the enzyme indicated that MADLS dominated

the data as the intensity of scattered light is proportional to the sixth power of the particle diameter and inversely proportional to the fourth power of the wavelength [41]. As the concentration of large aggregates increases, more light is scattered by DLS compared to the light absorbed by the aggregates during SEC. Such a correlation was not observed for BSA and the mAb due to the low resolution of the size ratio and concentration of the monomer and HMWS by MADLS.

Practical Relevance

Typically, SEC is a batch release method and DLS is a characterization method in the early stage of development, scale-up and technology transfer of drug products. Development and scale-up activities for biopharmaceutical drug products require several characterization tests with limited product material and time constraints. While DLS by itself may not provide all the information obtained by SEC and other analytical tests, it is employed as a batch-to-batch comparability method in tandem with other tests. Through this study, we suggest that this approach can be employed for the rapid screening of particle size, concentration and estimation of the level of aggregation in biopharmaceutical formulations provided the aggregates of the biologic are stable, well-resolved and reproducible during MADLS measurements. Moreover, the screening of these CQAs by MADLS during early-phase biopharmaceutical development can help in selecting samples for further analysis by SEC and other QC tests, thereby reducing the number of samples and experiments required for testing and analysis.

Conclusions

This study was able to assess the 3-in-1 capability of MADLS technology for the measurement of particle size, particle concentration and aggregation for 3 different protein modalities in tandem with UV–Vis spectroscopy and SEC. It was observed that the accuracy, resolution and reproducibility of MADLS measurements are dependent on the nature of the protein nanoparticle. Despite the different levels of polydispersity in the 3 protein solutions, a good calibration curve with an R^2 of >0.95 was obtained between the particle number concentration by MADLS and protein concentration by UV–Vis spectroscopy. In terms of the accuracy and precision of the measurements, key factors such as multiple scattering and particle number fluctuations are responsible for defining the operating particle concentration range. Additionally, restricted diffusion, electrostatic repulsion and reversible self-associations can also play a role in increasing the uncertainty in MADLS measurements. In terms of evaluating protein aggregation, MADLS provided better resolution and reproducibility for the multimodal distribution by the intensity of the enzyme. The observed quadratic correlation ($R^2=0.9938$) between MADLS and SEC for the enzyme and the approach provided in this study to assess the 3 CQAs can be employed for products with polydispersity similar to the enzyme. Overall, MADLS is a promising analytical technique that can be employed as an early-stage screening method for the analysis of different formulations and products prior to other analytical tests. While it may not qualify as a standalone QC release test, it can provide analysts and regulators with additional orthogonal data to complement traditional methods.

Supplementary Information The online version contains supplementary material available at https://doi.org/10.1208/s12249-023-02529-4.

Acknowledgements The authors would like to acknowledge and thank Tracey Carroll and Bryan Rellis for their support with SEC analyses, Warren Roche for his support with statistical analyses and Kevin O'Connor for his critical review of the manuscript.

Author Contribution Conceptualization: Ashutosh Sharma, Jason Beirne and Dikshitkumar Khamar. Data curation: Ashutosh Sharma. Formal analysis: Ashutosh Sharma, Jason Beirne and Dikshitkumar Khamar. Funding acquisition: Ashutosh Sharma and Helen Hughes. Methodology: Ashutosh Sharma and Jason Beirne. Project administration: Dikshitkumar Khamar and Helen Hughes. Resources: Dikshitkumar Khamar and Helen Hughes. Software: Ashutosh Sharma and Ciaran Maguire. Supervision: Jason Beirne, Dikshitkumar Khamar, Ambrose Hayden and Helen Hughes. Validation: Ashutosh Sharma, Jason Beirne and Dikshitkumar Khamar. Writing—original draft: Ashutosh Sharma. Writing—review and editing: Ashutosh Sharma, Jason Beirne, Dikshitkumar Khamar, Ciaran Maguire, Ambrose Hayden and Helen Hughes.

Funding The authors acknowledge the funding received from the South East Technological University (SETU), Waterford—Sanofi Waterford Co-fund PhD Scholarship Program (Ashutosh Sharma), the Irish Research Council—Enterprise Partnership Scheme (Project ID: EPSPG/2020/56), and the Higher Education Authority (HEA)—COVID-19 costed extension by the Department of Further and Higher Education, Government of Ireland.

Data Availability The authors confirm that the data supporting the findings of this study are available within the article and its supplementary information. Additional data that support the findings of this study (not included in this publication) are available from the corresponding author upon request.

Declarations

Competing Interests The authors declare no competing interests.

References

1. Wang W, Singh S, Zeng DL, King K, Nema S. Antibody structure, instability, and formulation. J Pharm Sci. 2007;96:1–26. https://linkinghub.elsevier.com/retrieve/pii/S0022354916321633. Accessed 4 Apr 2022.
2. Arakawa T, Prestrelski SJ, Kenney WC, Carpenter JF. Factors affecting short-term and long-term stabilities of proteins [Internet]. Adv Drug Deliv Rev. 2001. https://doi.org/10.1016/S0169-409X(00)00144-7.

3. Wang W, Roberts CJ. Protein aggregation – mechanisms, detection, and control. Int J Pharm. 2018;550:251–68. https://doi.org/10.1016/j.ijpharm.2018.08.043.
4. Declerck PJ. Biologicals and biosimilars: a review of the science and its implications. Generics Biosimilars Initiat J. 2012;1:13–6. http://gabi-journal.net/biologicals-and-biosimilars-a-review-of-the-science-and-its-implications.html. Accessed 1 Oct 2022.
5. Moussa EM, Panchal JP, Moorthy BS, Blum JS, Joubert MK, Narhi LO, et al. Immunogenicity of therapeutic protein aggregates [Internet]. J. Pharm. Sci. Elsevier B.V.; 2016. p. 417–30. https://doi.org/10.1016/j.xphs.2015.11.002.
6. Marianayagam NJ, Sunde M, Matthews JM. The power of two: protein dimerization in biology. https://doi.org/10.1016/j.tibs.2004.09.006.
7. Sharma A, Khamar D, Cullen S, Hayden A, Hughes H. Innovative drying technologies for biopharmaceuticals. Int J Pharm. Elsevier; 2021;121115. https://doi.org/10.1016/j.ijpharm.2021.121115.
8. Olson BJSC, Markwell J. Assays for determination of protein concentration. Curr Protoc Pharmacol. John Wiley & Sons, Ltd; 2007;38:A.3A.1-A.3A.29. https://onlinelibrary.wiley.com/doi/full/https://doi.org/10.1002/0471141755.pha03as38.
9. Knight MI, Chambers PJ. Problems associated with determining protein concentration: a comparison of techniques for protein estimations. Mol Biotechnol. 2003;23:19–28. https://pubmed.ncbi.nlm.nih.gov/12611266/. Accessed 27 Dec 2022.
10. FDA. Guidance for industry drug substance chemistry, manufacturing, and controls information [Internet]. 2010. https://www.fda.gov/media/69923/download. Accessed 9 Sep 2022.
11. Al-Ghobashy MA, Mostafa MM, Abed HS, Fathalla FA, Salem MY. Correlation between dynamic light scattering and size exclusion high performance liquid chromatography for monitoring the effect of pH on stability of biopharmaceuticals. J Chromatogr B Anal Technol Biomed Life Sci. 2017;1060:1–9. http://www.ncbi.nlm.nih.gov/pubmed/28578190. Accessed 12 May 2022.
12. Fekete S, Beck A, Veuthey JL, Guillarme D. Theory and practice of size exclusion chromatography for the analysis of protein aggregates. J Pharm Biomed Anal Elsevier. 2014;101:161–73. https://doi.org/10.1016/j.jpba.2014.04.011.
13. Patel BA, Gospodarek A, Larkin M, Kenrick SA, Haverick MA, Tugcu N, et al. Multi-angle light scattering as a process analytical technology measuring real-time molecular weight for downstream process control. MAbs. Taylor and Francis Inc.; 2018;10:1–6. https://doi.org/10.1080/19420862.2018.1505178.
14. Ramakrishna A, Prathap V, Maranholkar V, Rathore AS. Multi-wavelength UV-based PAT tool for measuring protein concentration. J Pharm Biomed Anal. Elsevier; 2022;207:114394. https://doi.org/10.1016/j.jpba.2021.114394.
15. Nitika N, Chhabra H, Rathore AS. Raman spectroscopy for in situ, real time monitoring of protein aggregation in lyophilized biotherapeutic products. Int J Biol Macromol Elsevier. 2021;179:309–13. https://doi.org/10.1016/j.ijbiomac.2021.02.214.
16. Pieters S, Vander Heyden Y, Roger JM, D'Hondt M, Hansen L, Palagos B, et al. Raman spectroscopy and multivariate analysis for the rapid discrimination between native-like and non-native states in freeze-dried protein formulations. Eur J Pharm Biopharm. Elsevier; 2013. p. 263–71. https://doi.org/10.1016/j.ejpb.2013.03.035.
17. Wang X, Esquerre C, Downey G, Henihan L, O'Callaghan D, O'Donnell C. Assessment of infant formula quality and composition using Vis-NIR, MIR and Raman process analytical technologies. Talanta. 2018;183:320–8. https://doi.org/10.1016/j.talanta.2018.02.080.
18. Zölls S, Tantipolphan R, Wiggenhorn M, Winter G, Jiskoot W, Friess W, et al. Particles in therapeutic protein formulations, Part 1: Overview of analytical methods. J Pharm Sci Elsevier. 2012;101:914–35. https://doi.org/10.1002/jps.23001.
19. Malvern Panalytical. Zetasizer Ultra [Internet]. 2022. https://www.malvernpanalytical.com/en/products/product-range/zetasizer-range/zetasizer-ultra. Accessed 15 Sep 2022.
20. Naiim M, Boualem A, Ferre C, Jabloun M, Jalocha A, Ravier P. Multiangle dynamic light scattering for the improvement of multimodal particle size distribution measurements. Soft Matter. 2015;11:28–32. https://pubs.rsc.org/en/content/articlehtml/2015/sm/c4sm01995d. Accessed 26 Oct 2021.
21. Bryant G, Abeynayake C, Thomas JC. Improved particle size distribution measurements using multiangle dynamic light scattering. 2. Refinements and applications. Langmuir. American Chemical Society ; 1996;12:6224–8. https://pubs.acs.org/doi/abs/https://doi.org/10.1021/la960224o.
22. Bryant G, Thomas JC. Improved particle size distribution measurements using multiangle dynamic light scattering. Langmuir. American Chemical Society; 1995;11:2480–5. https://pubs.acs.org/doi/pdf/https://doi.org/10.1021/la00007a028.
23. Weinbuch D, Cheung JK, Ketelaars J, Filipe V, Hawe A, Den Engelsman J, et al. Nanoparticulate impurities in pharmaceutical-grade sugars and their interference with light scattering-based analysis of protein formulations. Pharm Res. Springer New York LLC; 2015;32:2419–27. https://doi.org/10.1007/s11095-015-1634-1.
24. Corbett D, Bye JW, Curtis RA. Measuring nonspecific protein-protein interactions by dynamic light scattering. In: McManus JJ, editor. Protein self-assembly. Kildare, Ireland: Humana Press; 2019. p. 3–22. https://www.roma1.infn.it/~sciortif/PDF/2019/protein.pdf. Accessed 30 Dec 2022.
25. Markova N, Cairns S, Jankevics-Jones H, Kaszuba M, Caputo F, Parot J. Biophysical characterization of viral and lipid-based vectors for vaccines and therapeutics with light scattering and calorimetric techniques. Vaccines. 2022;10:49. https://www.mdpi.com/2076-393X/10/1/49/htm. Accessed 29 Dec 2022.
26. Bhattacharjee S. DLS and zeta potential – what they are and what they are not? J Control Release. 2016;235:337–51. https://doi.org/10.1016/j.jconrel.2016.06.017.
27. Malvern Panalytical. Multi-angle dynamic light scattering (MADLS) on the Zetasizer Ultra – how it works | Malvern Panalytical [Internet]. 2018. https://www.malvernpanalytical.com/en/learn/knowledge-center/technical-notes/TN180719HowItWorksMADLS.html. Accessed 22 June 2022.
28. Austin J, Minelli C, Hamilton D, Wywijas M, Jones HJ. Nanoparticle number concentration measurements by multi-angle dynamic light scattering. J Nanoparticle Res. Springer; 2020;22. https://doi.org/10.1007/s11051-020-04840-8.
29. Bhirde A, Chikkaveeraiah BV, Venna R, Carley R, Brorson K, Agarabi C. High performance size exclusion chromatography and high-throughput dynamic light scattering as orthogonal methods to screen for aggregation and stability of monoclonal antibody drug products. J Pharm Sci. Elsevier B.V.; 2020;109:3330–9. https://doi.org/10.1016/j.xphs.2020.08.013.
30. Cole L, Fernandes D, Hussain MT, Kaszuba M, Stenson J, Markova N. Characterization of recombinant adeno-associated viruses (rAAVs) for gene therapy using orthogonal techniques. Pharm. 2021;13:586. https://www.mdpi.com/1999-4923/13/4/586/htm. Accessed 22 June 2022.
31. Vogel R, Savage J, Muzard J, Camera G Della, Vella G, Law A, et al. Measuring particle concentration of multimodal synthetic reference materials and extracellular vesicles with orthogonal techniques: who is up to the challenge? J Extracell Vesicles. Wiley-Blackwell; 2021;10. https://doi.org/10.1002/jev2.12052.
32. Sahin Z, Demir YK, Kayser V. Global kinetic analysis of seeded BSA aggregation. Eur J Pharm Sci. Elsevier B.V.; 2016;86:115–24. https://doi.org/10.1016/j.ejps.2016.03.007.
33. Brookhaven Instruments. Absolute size exclusion chromatography of BSA - Brookhaven instruments [Internet]. 2019. https://www.

brookhaveninstruments.com/absolute-size-exclusion-chromatography-of-bsa/. Accessed 30 June 2022.
34. Jachimska B, Wasilewska M, Adamczyk Z. Characterization of globular protein solutions by dynamic light scattering, electrophoretic mobility, and viscosity measurements. Langmuir. American Chemical Society; 2008;24:6867–72. https://pubs.acs.org/doi/abs/https://doi.org/10.1021/la800548p.
35. Anton Paar. Dimerization of bovine serum albumin as evidenced by particle size and molecular mass measurement [Internet]. 2018. https://s3-eu-central-1.amazonaws.com/centaur-wp/theengineer/prod/content/uploads/2018/04/05161827/Bovine-serum-albumin-testing.pdf. Accessed 2 Feb 2022.
36. Malvern Panalytical. Influence of concentration effects and particle interactions on DLS analysis of bioformulations [Internet]. News Med Life Sci. 2014. https://www.news-medical.net/whitepaper/20141218/Influence-of-Concentration-Effects-and-Particle-Interactions-on-DLS-Analysis-of-Bioformulations.aspx. Accessed 18 Jul 2022.
37. Ragheb R, Nobbmann U. Multiple scattering effects on intercept, size, polydispersity index, and intensity for parallel (VV) and perpendicular (VH) polarization detection in photon correlation spectroscopy. Sci Rep. 2020;10:1–9. https://www.nature.com/articles/s41598-020-78872-4. Accessed 19 Feb 2022.
38. Hopcraft K, Chang P, Jakeman E, Walker J. Polarization fluctuation spectroscopy. In: Videen G, Yatskiv Y, Mishchenko M, editors. Photopolarimetry Remote Sens. Netherlands: Springer; 2005. p. 137–74. https://doi.org/10.1007/1-4020-2368-5_6.
39. Panchal J, Kotarek J, Marszal E, Topp EM. Analyzing subvisible particles in protein drug products: a comparison of dynamic light scattering (DLS) and resonant mass measurement (RMM). AAPS J. Springer New York LLC; 2014;16:440–51. https://doi.org/10.1208/s12248-014-9579-6.
40. von Bülow S, Siggel M, Linke M, Hummer G. Dynamic cluster formation determines viscosity and diffusion in dense protein solutions. Proc Natl Acad Sci U S A. National Academy of Sciences; 2019;116:9843–52. https://www.pnas.org/doi/abs/https://doi.org/10.1073/pnas.1817564116.
41. Zhu S, Ma L, Wang S, Chen C, Zhang W, Yang L, et al. Light-scattering detection below the level of single fluorescent molecules for high-resolution characterization of functional nanoparticles. 2014; https://pubs.acs.org/doi/full/https://doi.org/10.1021/nn505162u.